Articles

Physical Chemistry of Organic Eutectic and Monotectic: Hexamethylbenzene−Succinonitrile System

U. S. Rai and R. N. Rai

Chemistry Department, Banaras Hindu University, Varanasi-221005, India

Received October 5, 1998. Revised Manuscript Received July 29, 1999

A phase diagram of hexamethylbenzene−succinonitrile system, determined by the thaw−melt method, shows the formation of a eutectic and a monotectic with large miscibility gap in the system. The eutectic and the monotectic contain 0.150 and 0.996 mol fraction of succinonitrile, respectively, and the consolute temperature is 111.5 °C above the monotectic horizontal. Growth behavior of the eutectic, the monotectic, and the pure components, studied at different undercooling temperatures by measuring the rate of movement of solid−liquid interface in a capillary, suggests that the data obey the square relationship between growth velocity and the undercooling. Using enthalpy of fusion data, determined by the DSC method, entropy of fusion, enthalpy of mixing, size of the critical nucleus, interfacial energy, and excess thermodynamic functions were calculated. While the microstructures of the pure components, namely, hexamethylbenzene and succinonitrile show faceted and nonfaceted morphology, respectively, those of the eutectic and the monotectic give lamellar structures.

1. Introduction

To cater the needs of current civilization, the modern age of science demands materials with diverse properties. The fundamental understanding solidification and properties of polyphase alloys is the key to the technological development of novel materials with high strength, rigidity, and ductility at high temperatures for various applications. Chemistry of metal eutectics[1−3] and intermetallic compounds[4−6] is a potential area of investigation in metallurgy and materials science. However, metallic systems are not suitable for detailed investigations, as high transformation temperatures and wide differences in density of components pose serious problems in their experimentation. Due to low transformation temperature, ease in purification, transparency, wider choice of materials, and minimized convection effects, a number of research groups[7−10] have realized the importance of organic systems as a model for detailed investigation of the parameters which control the mechanism of solidification that decides the properties of materials. The above-mentioned inherent physical properties of the organic compounds and simplicity of their experimentation have prompted a number of researchers[11−14] to work on some physicochemical aspects of organic eutectics, monotectics, and molecular complexes.

Eutectic reaction is characterized by the isothermal decomposition of a liquid phase into two solid phases. On the other hand, monotectic reaction involves the breakdown of a liquid phase into a solid phase and a liquid phase. Because of a limited choice of materials and experimental difficulties associated with the miscibility gap, less attention has been focused to monotectic alloys. However, the past decade has witnessed several articles[15−18] that explain various interesting phenomena during the solidification of monotectic alloys. The role of wetting behavior, interfacial energy, thermal conductivity and buoyancy in a phase-separation process has been the subject of great discussion. Succinonitrile (SCN), a material of low entropy of fusion, simulates the metallic solidification and hexamethylbenzene (HMB), a material of high entropy of fusion simulates the nonmetallic solidification. As such the

(1) Elliott, R. *Eutectic Solidification Processing*; Butterworths: London 1983.
(2) Glazer, J. *Int. Mater. Rev.* **1995**, *40*, 65.
(3) Lee, J. H.; Verhoeven, J. D. *J. Cryst. Growth* **1994**, *143*, 86.
(4) Rzyman, K.; Moser, Z.; Watson, R. E.; Weinert, M. *J. Phase Equilib.* **1996**, *17*, 173.
(5) Trivedi, R.; Kurz, W. *Int. Mater. Rev.* **1994**, *32*, 49.
(6) Tewari, S. N. *Metall. Trans.* **1987**, *18A*, 525.
(7) Hunt, J. D.; Jackson, K. A. *Trans. Met. Soc. AIME* **1966**, *236*, 1129.
(8) Podolinsky, V. V.; Taran, N. Y.; Drykin, V. G. *J. Cryst. Growth* **1989**, *96*, 445.
(9) Yasuda, H.; Ohnaka, I.; Matasunaga, Y.; Shiohara, Y. *J. Cryst. Growth* **1996**, *158*, 128.
(10) Grugel, R. N.; Poorman, R. *Mater. Sci. Forum* **1989**, *50*, 89.
(11) Pigon, K.; Krajewska, A. *Thermochim. Acta* **1982**, *58*, 58.
(12) Glicksman, M. E.; Singh, N. B.; Chopra, M. *Manuf. Space* **1983**, *11*, 207.
(13) Rastogi, R. P.; Singh, N. B.; Dwivedi, K. D. *Ber. Bunsen-Ges. Phys. Chem.* **1981**, *85*, 85.
(14) Singh, N. B.; Singh, N. N.; Laidlaw, R. K. *J. Solid State Chem.* **1987**, *71*, 530.
(15) Herlach, D. M.; Cochrane, R. F.; Egry, I.; Fecht, H. J.; Greer, A. L. *Int. Mater. Rev.* **1993**, *38*, 273.
(16) Sandlin, A. C.; Andrews, J. B.; Curreri, P. A. *Metall. Trans.* **1988**, *18A*, 2665.
(17) Derby, B.; Favier, J. J. *Acta Metall.* **1983**, *7*, 1123.
(18) Ecker, A.; Frazier, D. O.; Alexander, J. I. D. *Metall. Trans.* **1989**, *20A*, 2517.

10.1021/cm9806937 CCC: $18.00
Published on Web 10/27/1999

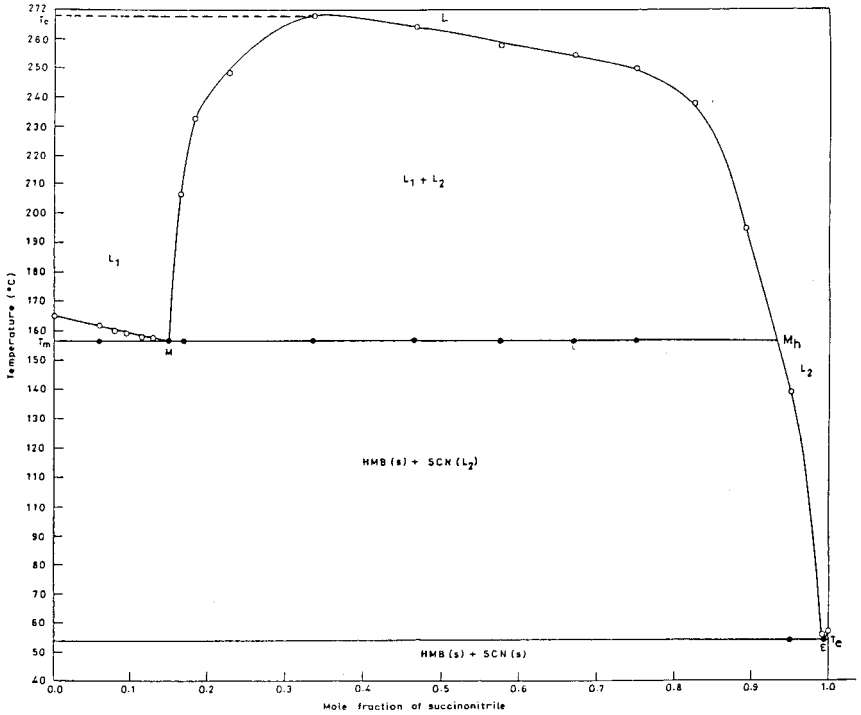

Figure 1. Phase diagram of hexamethylbenzene-succinonitrile system: ○, melting temperature; ●, thaw temperature.

HMB−SCN system may be chosen as a suitable analogue of metal−nonmetal systems such as Al−Si and Al−Be. In the present article, data on phase diagram, growth behavior, thermochemistry, and microstructure of the HMB−SCN system have been reported.

2. Experimental Section

2.1. Materials and Purification. Succinonitrile obtained from Aldrich-Chemie, Germany was purified by repeated distillation under reduced pressure. On the other hand, hexamethylbenzene (Ega-Chemie, Germany) was purified by repeated crystallization. The melting points of hexamethylbenzene and succinonitrile were found to be 165.0 and 56.5 °C, respectively, which match within ±0.5 °C with the respective values reported in the literature.[19] This ensures the purity of these compounds used in the present investigation.

2.2. Phase Diagram. The phase diagram of the HMB−SCN system was determined by the thaw−melt method.[20] In this method, mixtures of the two components covering the entire range of composition were prepared in different long-necked test tubes. These mixtures were homogenized by repeating a method of alternate melting in silicone oil followed by chilling in ice, several times. The test tubes were broken and thawing and melting temperatures of each mixture were determined using a Toshniwal melting point apparatus (capillary melting tube apparatus) equipped with a thermometer which could read correctly up to 0.5 °C.

2.3. Growth Kinetics. The linear velocity of crystallization of pure components, eutectic, and monotectic was determined by measuring the rate of movement of growth front in a capillary using the procedure described earlier.[21−22] A Pyrex glass tube (15 cm long with inner diameter 0.5 cm) in the U form was washed and dried before filling it with the test sample to determine the linear velocity of crystallization. The tube containing the molten sample, free from air bubbles, was mounted on a wooden board with a fitted scale. The entire assembly was then kept in a thermostat-maintained oil bath at a temperature slightly above the melting point of the material taken in the tube. The temperature of the bath was allowed to fall and set at a temperature a few degrees below the melting point. At each temperature, when the tube attained the temperature of the bath, a seed crystal of the same substance was added to one end of the tube for nucleation to set in. As soon as the seed crystal was added, nucleation followed by crystallization took place linearly in the tube and the time required for the crystal front to travel a predetermined distance (monitored by a travelling microscope) was noted with the help of a stop watch. As expected, at a fixed undercooling, the distance increases linearly with time.

2.4. Enthalpy of Fusion. The heats of fusion of pure components, eutectic, and monotectic were determined[23] by a differential scanning calorimeter, Mettler DSC-4000 system. Indium sample was used to calibrate the system, and amount of test sample and heating rate were about 5 mg and 10 °C min^{-1}, respectively, for each estimation. The values of enthalpy of fusion are reproducible within ±1.0%.

2.5. Microstructure. Microstructures of pure components, eutectic, and monotectic were recorded[22,24−25] by taking small amount of sample on a well washed and dried glass slide and placing it in an oven maintained at a temperature slightly above the melting point of the sample. On complete melting, a coverslip was slipped over the melt, and the slide was allowed to cool to obtain a supercooled liquid. The melt was nucleated with a seed crystal of the same composition and care was taken to have unidirectional freezing. The slide with the solid was then placed on the platform of a Leitz Laborlux D optical microscope. Different regions were viewed and photographs of suitable magnification were taken with the help of camera attached with the microscope.

3. Results and Discussion

3.1. Phase Diagram. The phase diagram of the HMB−SCN system (Figure 1), expressed in terms of

(19) Dean, J. A. *Lange's handbook of chemistry*; McGraw-Hill Book Company: New York 1985.
(20) Rai, U. S.; Mandal, K. D. *Mol. Cryst. Liq. Cryst.* **1990**, *182A*, 387.
(21) Rai, U. S.; Mandal, K. D. *Bull. Chem. Soc. Jpn.* **1990**, *63*, 1496.
(22) Singh, N. B.; Singh, N. B. *Krist. Technik.* **1978**, *13*, 1175.
(23) Rai, U. S.; Mandal, K. D.; Singh, N. P. *J. Therm. Anal.* **1989**, *35*, 1687.
(24) Rastogi, R. P.; Rastogi, V. K. *J. Cryst. Growth* **1969**, *5*, 345.
(25) Rai, U. S. *J. Cryst. Growth* **1994**, *144*, 291.

composition and temperature, clearly shows that HMB forms a monotectic (0.150 mol fraction of SCN) and a eutectic (0.996 mol fraction of SCN), the upper consolute temperature being 111.5 °C above the monotectic horizontal. The two components are miscible in all proportions above a critical temperature, T_C. Below this temperature and between certain composition limits indicated in the figure by $L_1 + L_2$, two immiscible liquids are produced. When a liquid of monotectic composition (M) is cooled through the monotectic horizontal (T_m), the monotectic reaction occurs and a liquid L_1 rich in HMB decomposes into a solid-phase rich in HMB and a liquid-phase L_2 rich in SCN. The monotectic reaction, at the monotectic temperature can be written as

$$L_1 \rightleftharpoons S_1 + L_2$$

L_1 (rich in HMB) $\rightleftharpoons$

S_1 (rich in HMB) + L_2 (rich in SCN)

On the other hand, when a liquid (L_2) of eutectic composition is cooled below the eutectic horizontal T_E, the eutectic liquid decomposes to give two solids S_1 and S_2 as

$$L_2 \rightleftharpoons S_1 + S_2$$

L_2 (rich in SCN) $\rightleftharpoons$

S_1 (rich in HMB) + S_2 (rich in SCN)

Evidently, when a liquid L with its composition in the liquid immiscibility gap region is cooled, above the monotectic horizontal, it gives two liquids as

$$L \rightarrow L_1 + L_2$$

The eutectic, monotectic and the critical solution temperatures are 54.5, 156.5, and 268.0 °C, respectively.

3.2. Growth Kinetics. Growth behavior of eutectics of metal and of organic origins has been studied by many workers,[1,26] and the data are verified by several experiments. In addition, mechanism of eutectic solidification is explained by the very successful Jackson−Hunt theory[7] reported in 1966 which was later on verified by a different group of workers in this area. On the other hand, study of growth behavior of monotectic is limited to only a few systems and, to date, no successful theory has been proposed to explain the mechanism of monotectic solidification. However, some workers[17,27] have successfully checked the validity of the Jackson−Hunt theory for monotectic systems also. In this theory the kinetic undercooling was neglected, considering it to be very small in magnitude in comparison to undercoolings due to the composition and curvature. SCN is a low enthalpy of fusion material, and HMB melts with high enthalpy of fusion resulting in very large value of kinetic undercooling. This requires more driving force for nucleation to take place. In view of this, linear velocity of crystallization (v) of the pure components, the eutectic, and the monotectic was determined at different undercooling temperatures (ΔT).

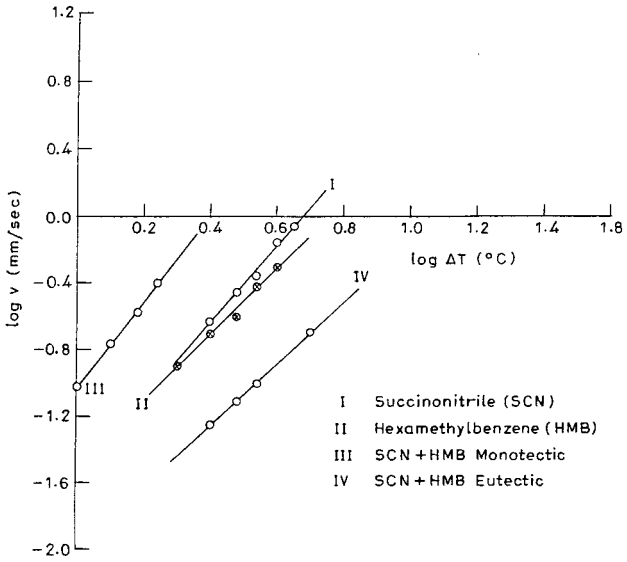

Figure 2. Linear velocity of crystallization of hexamethylbenzene, succinonitrile, and their eutectic and monotectic.

Table 1. Value of *u* and *n* for Pure Components, Eutectic, and Monotectic

materials	n	$u \times 10^2$ (mm S^{-1} deg^{-1})
hexamethylbenzene (HMB)	1.9	3.2
succinonitrile (SCN)	2.3	2.8
HMB−SCN monotectic	2.6	9.6
HMB−SCN eutectic	2.0	1.0

The growth velocity is related to the undercooling by the equation[28]

$$v = u(\Delta T)^n \quad (1)$$

where u and n are constants depending on the nature of materials involved. Equation 1 can be expressed in logarithmic form as given in

$$\log v = \log u + n \log \Delta T \quad (2)$$

If a graph is plotted between log v on y axis and log ΔT on x axis, a straight line should be obtained for different materials of the HMB−SCN system. The straight lines for different materials of the HMB−SCN system are shown in Figure 2, and the values of n and u are given in Table 1. The values of n being quite close to 2 suggest square relationship between the growth velocity and the undercooling. Two theories[29] have been advanced for the growth mechanism which predict that $n = 2$. While one theory is based on the conduction of heat from the tip of the crystal to the surrounding liquid, the other is based on the screw dislocation mechanism of growth. The deviations in the value of n from 2, observed in some cases, may be due to difference in bath temperature and the temperature of the growing interface. It is due to release of latent heat which would cause the interface to attain a temperature higher than that of the bulk of the liquid representing bath temperature.

It may be emphasized that the values of log u are the intercept of straight lines with the log v axis in the Figure 2, when log $\Delta T = 0$. It can be concluded from

(26) Rai, U. S.; Singh, O. P.; Singh, N. B. *J. Chim. Phys.* **1987**, *84*, 483.
(27) Singh, N. B.; Rai, U. S.; Singh, O. P. *J. Cryst. Growth* **1985**, *71*, 353.
(28) Rai, U. S.; Shekhar, H. *Mol. Cryst. Liq. Cryst.* **1992**, *226*, 217.
(29) Rastogi, R. P.; Singh, N. B.; Singh, Narsingh B.; Dwivedi, K. D. *Indian J. Chem.* **1979**, *17A*, 431.

Table 2. Heat of Fusion and Entropy of Fusion

materials	heat of fusion (kJ mol^{-1})	entropy of fusion (J mol^{-1} K^{-1})
hexamethylbenzene (HMB)	19.6	44.8
succinonitrile (SCN)	3.7	11.2
HMB−SCN monotectic (experimental)	17.1	39.4
HMB−SCN monotectic (by mixture law)	17.2	
HMB−SCN eutectic (experimental)	3.4	10.4
HMB−SCN eutectic (by mixture law)	3.8	

the values of u (Table 1) that while growth velocity of the eutectic is lower than those of the components, in the case of monotectic it is higher than those of the components. These results may be explained on the basis of the mechanism reported earlier.[28] Accordingly, the solidification begins with the nucleation of one of the phases. This would grow until the surrounding liquid becomes rich in the other component, and a stage is reached when second phase also starts nucleating. Now, there are two possibilities. Either two phases may grow side-by-side or there may be alternate nucleation of two phases. While the former explains the higher growth rate of eutectics than those of the components, the latter explains the lower growth rate of the eutectics. The value of u of eutectic being lower than those of the components suggests that there is alternate nucleation of two phases involved. It is evident from the table that growth rate of monotectic is much higher than those of the components and also than that of the eutectic at a particular undercooling. This may be due to the higher diffusion rate of the components in the liquid phase present in the monotectic. It is also due to the difference in heat flow pattern of the monotectic from that of the eutectic.

3.3 Thermochemistry. *3.3.1. Enthalpy of Fusion.* The idea about mechanism of crystallization, microstructure, structure of eutectic melt, and nature of interaction between two components forming the eutectic and the monotectic can be obtained from a knowledge of their heat of fusion data. The experimental values of enthalpy of fusion, determined by the DSC method, are reported in Table 2; the percentage error in the values being ±1.0. For the purpose of comparison, the value of enthalpy of fusion of eutectic calculated by the mixture law is also given in the same table. If a eutectic is a simple mechanical mixture of two components involving no heat of mixing or any type of association in the melt, the heat of fusion can simply be given by the mixture law[28]

$$(\Delta_f h)_e = x_1 \cdot \Delta_f h_1^\circ + x_2 \cdot \Delta_f h_2^\circ \qquad (3)$$

where x and $\Delta_f h$ are the mole fraction and the heat of fusion, respectively, of the component indicated by the subscript. But when a solid eutectic melts, there is a considerable possibility of association and heat of mixing, both causing violation of the mixture law. It is evident from the table that the calculated value of heat of fusion is higher than the experimental one by 0.4 kJ mol^{-1}. Thus, the enthalpy of mxing ($\Delta_m H$), which is the difference between the experimental and the calculated values of heat of fusion, is −0.4 kJ mol^{-1}. Thermochemical studies[30] suggest that the structure of a binary eutectic melt depends on the sign and magnitude of heat of mixing. As such, three types of structures are suggested; quasi-eutectic for $\Delta_m H > 0$, clustering of molecules for $\Delta_m H < 0$ and molecular solution for $\Delta_m H = 0$. The negative value of $\Delta_m H$ for the eutectic suggests clustering of molecules in the binary melt. The entropy of fusion values, calculated by dividing enthalpy of fusion by absolute temperature corresponding to melting point of different materials (Table 2), being positive suggest that the entropy factor, in all cases, favors the melting process.

Table 3. Interfacial Energy of Hexamethylbenzene, Succinonitrile, and Their Eutectic and Monotectic

parameter	value (erg cm^{-2})
σ_{SL_2} (SCN)	9.3
σ_{SL_1} (HMB)	32.5
$\sigma_{L_1L_2}$ (HMB−SCN)	7.0
σ_E (HMB−SCN)	9.4

3.3.2. Size of Critical Nucleus and Interfacial Energy. When a melt is cooled below its melting temperature, the liquid phase does not solidify spontaneously. This is because of the fact that below equilibrium temperature the melt contains large number of clusters of molecules of different sizes. So long as the clusters are all below the critical size,[31] they cannot grow to form crystals and so no solid is formed. The critical size (γ^*) of nucleus is related[32] to interfacial energy (σ) by the equation

$$\gamma^* = \frac{2\sigma T_m}{\Delta_f H \cdot \Delta T} \qquad (4)$$

where T_m, $\Delta_f H$, and ΔT are melting temperature, heat of fusion, and degree of undercooling, respectively. An estimate of the interfacial energy is given by the expression

$$\sigma = \frac{C \cdot \Delta_f H}{(N)^{1/3} \cdot (V_m)^{2/3}} \qquad (5)$$

where N is the Avogadro number, V_m is the molar volume, and parameter C lies between 0.30 and 0.35. The values of interfacial energy calculated using eq 5 are reported in Table 3. The size of critical nucleus for the pure components, the eutectic and the monotectic is reported in Table 4. It is evident from the data that for a given material, the size of the critical nucleus decreases with an increase in undercooling. This is due to the fact that at increased undercooling the bulk free energy available for the phase transformation is increased, thereby lowering the total barrier height for nucleation. Consequently, smaller thermodynamic fluctuations can, with statistical certainty, eventually form a viable nucleus of size greater than the critical.

3.3.3. Excess Thermodynamic Functions. The deviation from ideal behavior can best be expressed in terms of excess thermodynamic functions, namely, excess free

(30) Singh, N.; Singh, Narsingh B.; Rai, U. S.; Singh, O. P. *Thermochim. Acta* **1985**, *95*, 291.
(31) Christian, J. W. *The theory of phase transformation in metals and alloys*; Pergamon Press: Oxford, 1965.
(32) Rai, U. S.; Shekhar, H. *Cryst. Res. Technol.* **1994**, *29*, 551.

Table 4. An Estimate of Critical Size of Nucleus at Different Undercoolings

undercooling ΔT (°C)	critical radius × 10^8 (cm)		
	HMB	SCN	eutectic
1.0			18.2
1.3			14.5
1.5			12.1
1.8			10.4
2.0	7.3		
2.5	5.8	6.7	
3.0	4.8	5.6	
3.5	4.2	4.8	
4.0	3.6	4.2	
4.5		3.7	

Table 5. Excess Thermodynamic Functions for the Eutectic

material	g^E (J mol^{-1})	h^E (k J mol^{-1})	s^E (J mol^{-1} K^{-1})
HMB−SCN eutectic	28.5	−1.5	−4.6

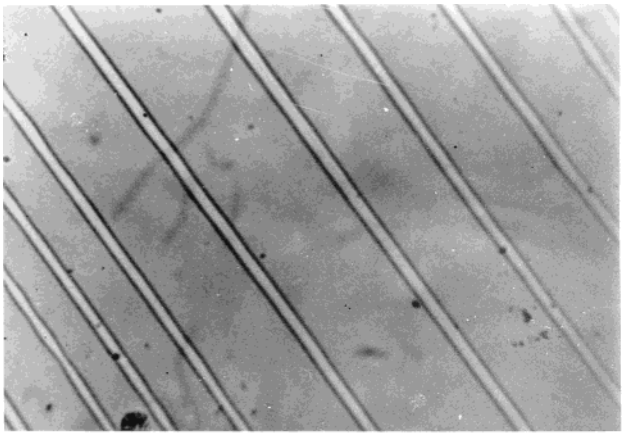

Figure 3. Lamellar microstructure of eutectic × 600 (at low growth rate).

energy (g^E), excess entropy (s^E), and excess enthalpy (h^E), which give a quantitative idea about the nature of molecular interactions. In general, it is defined as the difference between a thermodynamic function of mixing for a real system and the corresponding value for an ideal system at the same temperature and pressure. The thermodynamic functions can be calculated using the following equations:[33]

$$g^E = RT(x_1 \ln \gamma_1^1 + x_2 \ln \gamma_2^1) \quad (6)$$

$$s^E = -RT^2\left(x_1\frac{\partial \ln \gamma_1^1}{\partial T} + x_2\frac{\partial \ln \gamma_2^1}{\partial T}\right) \quad (7)$$

$$h^E = -R\left(x_1 \ln \gamma_1^1 + x_2 \ln \gamma_2^1 + x_1T\frac{\partial \ln \gamma_1^1}{\partial T} + x_2T\frac{\partial \ln \gamma_2^1}{\partial T}\right) \quad (8)$$

Evidently, to calculate the excess functions, the activity coefficient and its variation with temperature are required. While activity coefficient, γ_i, can be calculated using the equation

$$-\ln(x_1^1 \gamma_1^1) = \frac{\Delta_f h_i^\circ}{R}(T_e^{-1} - T_i^{-1}) \quad (9)$$

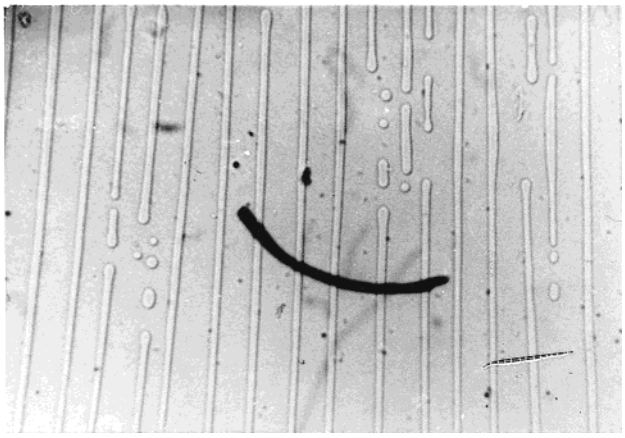

Figure 4. Lamellar microstructure of eutectic × 600 (at high growth rate).

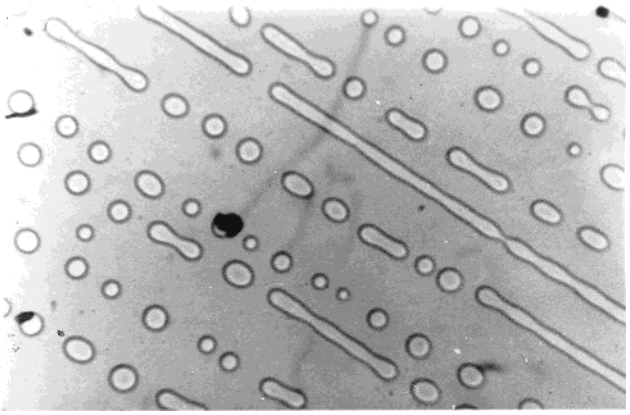

Figure 5. Broken lamellar microstructure of eutectic × 600 (at high growth rate).

where x_1^1, $\Delta_f h_i^\circ$, T_i°, and T_e are mole fraction, enthalpy of fusion and melting point of component i and T_e is the eutectic temperature, respectively, its variation with temperature can be calculated by differentiating eq 9 and using it as given earlier.[33] The values of g^E, h^E, and s^E are reported in Table 5. The positive values of excess free energy indicate that there is associative interaction between like molecules. The negative values of h^E and s^E correspond to the positive value of g^E confirming thereby the conclusion based on excess free energy.

3.4. Microstructure. In general, microstructure gives shape, size, and distribution of phases, and these factors play a very significant role in deciding mechanical, electrical, magnetic, and optical properties of materials. Thermal conductivity, entropy of fusion, and structure of solid−liquid interface are material-related properties and undercooling, growth velocity, and temperature gradient along interface are physical parameters, which are of immense importance to control the mechanism of microstructure. The shape that a crystal adopts in the melt after nucleation is controlled by the way in which molecules are added on to the solid−liquid interface.[34,35] Depending on the entropy of fusion of a material,[36] the growing interface may be either rough and noncrystalline in character or atomically smooth and crystalline. The undercooling of the interface pro-

(33) Rai, U. S.; Singh, O. P.; Singh, N. P.; Singh, Narsingh B. *Thermochim. Acta* **1983**, *71*, 373.
(34) Rai, U. S.; Shekhar, H. *Thermochim. Acta* **1991**, *186*, 131.

vides the driving force of the kinetic process in the direction of freezing, and its magnitude decides the rate of growth.

3.4.1. Microstructure of Eutectic. The microstructures of eutectic (Figures 3−5) clearly show its lamellar type of growth. In Figure 3, the lamellar distance is large in comparison to that in Figure 4. This is due to higher growth rate in the latter in comparison to the former. This is justified[36] by the fact that in lamellar growth, the lamellar distance is inversely proportioal to the growth rate. This is also justified by the lamellar faults observed in Figure 4. There may be two reasons[27] for this fault: (a) The pocket drops slowly backward from the interface and becomes unstable. This situation enhances the growth of other components terminating the lamellae. (b) Termination of the lamellae may be due to the change in composition at the interface, resulting from the effect of fluctuation in growth rate on the boundary layer. This can manifest itself in the overgrowth and pinching off of one of the components at the growing interface. The microstructure in Figure 5 clearly shows the tendency of change of lamellar growth into broken lamellar growth at a high growth rate. When growth rate is slow, the reaction site has enough time to form spheres. Elongated spheres or rod-type structures are observed in the figure when growth rate is high.

3.4.2. Microstructure of Monotectic. The general features (Figures 6 and 7) are quite similar to those of eutectics. In Figure 6, the interlamellar distance is higher than that in Figure 7. This is again due to high growth rate in Figure 7, in comparison to that in Figure 6. Figure 7 also shows a well-arranged array of droplets. When liquid (L_1) is allowed to cool below the monotectic temperature (T_m), solid HMB deposits. As a result the liquid adjacent to the interafce is enriched with SCN, owing to solute rejection, and becomes supersaturated with respect to SCN; droplets of SCN (L_2) then nucleates to relieve the supersaturation. Whether droplets nucleate in the melt or on the solid−liquid interface depends on the relative magnitude of the three interfacial energies, namely, σ_{SL_1}, σ_{SL_2}, and $\sigma_{L_1L_2}$. The interfacial energy $\sigma_{L_1L_2}$, was calculated using an equation reported earlier.[37] From the data reported in Table 3, it is evident that the Cahn wetting condition can be successfully applied to the present system. Accordingly,

$$\sigma_{SL_1} < \sigma_{SL_2} + \sigma_{L_1L_2}$$

Thus, the HMB−SCN liquid (L_1) wets the solidified HMB perfectly, and SCN-rich droplets (L_2) will be surrounded by the HMB−SCN liquid. Under this condition, there is the possibility of capillary instability of the type in Al−Bi system.[38] If the cell depths are greater than the droplet circumference, capillary instabilities will develop SCN droplets and they will pinch off into spheres. HMB-rich liquid subsequently solidifies behind these spheres. Repitition of this process produces very well arranged array of spheres observed in Figure 7.

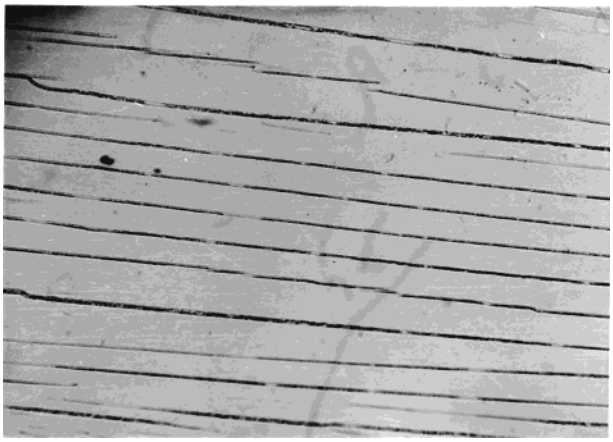

Figure 6. Lamellar microstructure of monotectic × 600 (at low growth rate).

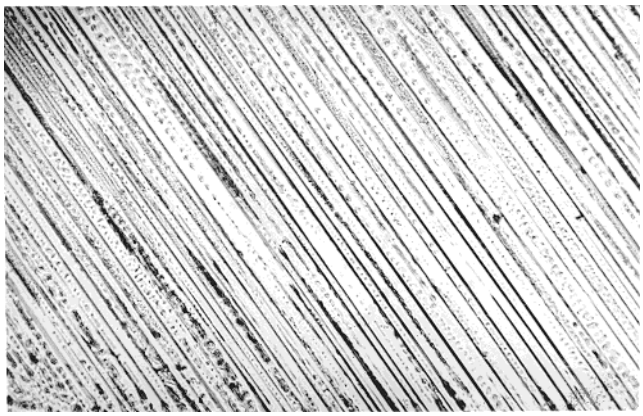

Figure 7. Broken lamellar microstructure of monotectic × 600 (at high growth rate).

Acknowledgment. Thanks are due to CSIR, New Delhi for financial assistance.

CM9806937

(35) Chadwick, G. A. *Metallography of phase transformation*; Butterworth: London, 1972; pp 86−158.
(36) Hunt, J. D.; Jackson, K. A. *Trans. Met. Soc. AIME* **1966**, *236*, 843.
(37) Good, R. *Ind. Eng. Chem.* **1970**, *62*, 54.
(38) Schafer, C.; Johnston, M. H.; Parr, R. A. *Acta Metall.* **1983**, *31*, 1229.